RSC Pharmaceutics

ROYAL SOCIETY OF CHEMISTRY

PAPER

View Article Online
View Journal | View Issue

Cite this: *RSC Pharm.*, 2025, **2**, 1125

Release performance and crystallization of racemic and enantiopure praziquantel amorphous solid dispersion in various media†

Benedito Roberto de Alvarenga Junior and Lynne S. Taylor *

Praziquantel (PZQ) is the first-line treatment for schistosomiasis, but its low aqueous solubility and extensive first-pass metabolism limit PZQ's bioavailability. Furthermore, the commercial formulation of PZQ includes the inactive (*S*)-PZQ enantiomer, which causes unwanted side effects and a bitter taste. This work aimed to evaluate the impact of chirality on PZQ's performance in amorphous solid dispersion (ASD) formulations prepared from both racemic and the active (*R*)-PZQ enantiomer, with additional studies on polymer type and processing method. ASDs of (*R*,*S*)-PZQ and (*R*)-PZQ at 30% drug loading were prepared with HPMCAS MF and HPMC E5 *via* solvent evaporation (SE) and hot-melt extrusion (HME). Release testing was conducted in aqueous media with different pH values and in biorelevant media simulating fasted- and fed-state conditions. Results demonstrated that ASDs significantly enhanced PZQ concentrations, with the amorphous solubility being up to 8-fold higher than that of the corresponding crystalline form. HPMCAS-based ASDs showed pH-dependent release, with poor release at gastric pH but achieving near-complete release with crystallization inhibition at intestinal pH conditions, while HPMC-based ASDs exhibited faster gastric release but reduced stability due to crystallization, which was confirmed by polarized light microscopy (PLM) and powder X-ray diffraction (PXRD). (*R*)-PZQ-HPMCAS ASDs outperformed (*R*,*S*)-PZQ-HPMCAS ASDs in simple media at pH 6.5 at high target concentration, which was attributed to a slightly higher amorphous solubility. However, both ASDs exhibited comparable release in fasted-state media due to bile salt-enhanced solubility. PZQ-ASDs showed crystallization when evaluated in FeSSIF-V2 and did not release well. Different processing methods minimally affected release profiles, highlighting HME's potential as a scalable, solvent-free method. These findings suggest that (*R*)-PZQ-HPMCAS is a promising alternative to commercial racemic PZQ formulations, potentially reducing side effects and improving patient compliance through allowing for a reduced pill burden.

Received 23rd April 2025,
Accepted 3rd July 2025

DOI: 10.1039/d5pm00117j

rsc.li/RSCPharma

1. Introduction

Schistosomiasis is a tropical disease caused by trematode worms of the genus *Schistosoma* that occurs in regions where water is contaminated or sanitation conditions are inadequate.[1,2] According to the World Health Organization (WHO), it is estimated that more than 250 million people worldwide required preventive treatment in 2021.[3] Currently, praziquantel (PZQ) is an anthelmintic drug recommended as the first-line treatment for all types of schistosomiasis and is also included in the WHO Model List of Essential Medicines for the treatment of both adults and children.[3,4]

PZQ belongs to Biopharmaceutics Classification System (BCS) class II and is characterized by high permeability and low solubility (0.4 mg mL^{-1} in water at 25 °C), which results in a slow dissolution rate in the gastrointestinal (GI) tract and consequently low bioavailability.[5–7] Furthermore, PZQ undergoes an extensive first-pass effect metabolism, converting into inactive metabolites rapidly.[6,8–10] In this context, it is necessary to administer a high drug dosage, usually 20 mg kg^{-1} three times a day at intervals of 4 to 6 hours or as a single dose of 40 mg kg^{-1} for preventive chemotherapy.[11,12] Therefore, investigations are warranted to obtain formulations with enhanced solubility and bioavailability to decrease the PZQ therapeutic dose and, thereby, the tablet size, which is difficult to swallow, in particular for pediatric treatment.

PZQ [2-(cyclohexylcarbonyl)-1,2,3,6,7,11*b*-hexahydro-4*H*-pyrazino[2,1*a*]isoquinolin-4-one] is commercially available in tablet form as the innovator product Biltricide®, as well as various generic versions, and is dosed as a crystalline racemic mixture at a proportion of 1 : 1.[12,13] The (*R*)-PZQ enantiomer is

Department of Industrial and Molecular Pharmaceutics, College of Pharmacy, Purdue University, West Lafayette, Indiana 47907, USA. E-mail: lstaylor@purdue.edu; Fax: +765-494-6545; Tel: +765-496-6614

† Electronic supplementary information (ESI) available. See DOI: https://doi.org/10.1039/d5pm00117j

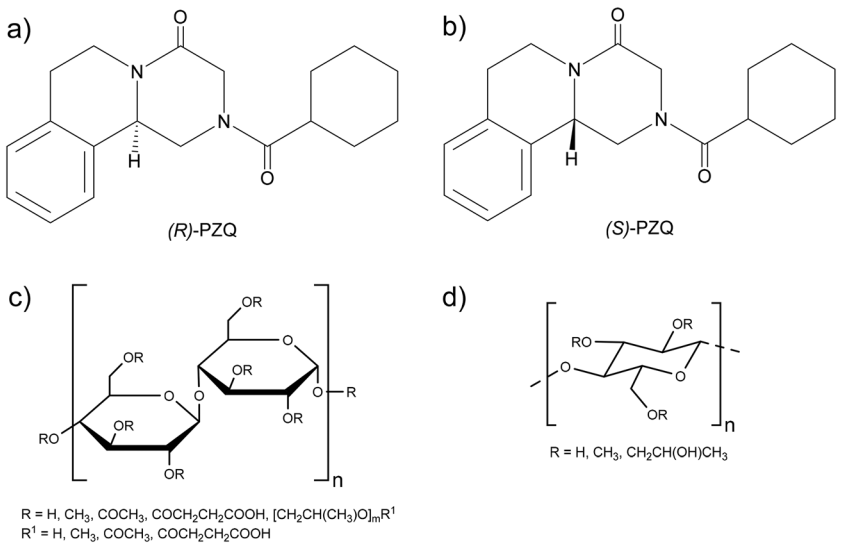

Fig. 1 Chemical structures of (*R*)-PZQ (a), (*S*)-PZQ (b), HPMCAS (c), and HPMC (d).

responsible for the pharmacological activity, while the (*S*)-PZQ enantiomer has little or no antischistosomal action and provides a bitter taste along with side effects such as abdominal pain, fever, nausea, and vomiting.[8,14–16] Given the drawbacks associated with PZQ, a possible way of overcoming its low bioavailability is to increase PZQ solubility through amorphous solid dispersion (ASD).

ASDs consist of a homogeneous dispersion of the active pharmaceutical ingredient (API) in an inert excipient carrier in the amorphous state.[17,18] Since the API is in the amorphous state within an ASD formulation, no energy is necessary to break the crystal lattice, which increases the apparent water solubility, dissolution rate, and bioavailability.[19–21] Moreover, improvements in release and wettability due to the presence of a hydrophilic polymer are also factors that may contribute to enhanced drug release.[22,23]

Several studies have reported release studies of PZQ-ASD formulations prepared by solvent evaporation (SE),[24–28] the fusion method,[29] co-precipitation,[29,30] co-grinding,[31] spray drying,[32] and hot-melt extrusion (HME).[33,34] Most of these studies performed dissolution testing in simple aqueous media. It is also valuable to evaluate the dissolution profile in media that simulate fasted and fed states, in particular for poorly soluble compounds.[35] While the impact of biorelevant media has been studied for a formulation containing crystalline PZQ,[36] to the best of our knowledge, no studies have explored the influence of biorelevant media on the release rate of PZQ-ASD formulations. In addition, there are limited studies on the release properties of ASDs prepared with the pharmacologically active (*R*)-PZQ enantiomer.

Therefore, this work aims to evaluate the impact chirality on the PZQ release behavior from ASDs in aqueous media at different pH conditions and in fasted/fed-state simulated GI fluids (FaSSGF, FaSSIF, and FeSSIF-V2), while also varying polymer type and processing method. ASDs of (*R*,*S*)-PZQ and (*R*)-PZQ at 30% drug loading (DL) were prepared with HPMCAS MF and HPMC E5 LV *via* solvent evaporation (SE) and hot-melt extrusion (HME). Crystallization during release studies was analyzed using polarized light microscopy (PLM) and powder X-ray diffraction (PXRD). Fig. 1 shows the chemical structure of (*R*)-PZQ, (*S*)-PZQ, and polymers.

2. Experimental section

2.1. Materials

(*R*)-PZQ (purity 99.9%) was sourced from Tongli Biomedical Co. (Zhangjiagang, China).

(*R*,*S*)-PZQ (purity 95%+) was sourced from ChemShuttle (Burlingame, CA). Hydroxypropyl methylcellulose acetate succinate MF grade (HPMCAS-MF; AQOAT AS-MF, Shin-Etsu, Tokyo, Japan) and hydroxypropyl methylcellulose E5 LV grade (HPMC; Methocel E5 Premium LV, The Dow Chemical Company, Midland, MI) were the polymers used in this work.

Table 1 Solution composition of fasted and fed-stated simulated media[35,38]

	Fasted state		Fed state
Composition	FaSSGF	FaSSIF	FeSSIF-V2
SIF powder (g)	0.06	2.24	9.76
Sodium taurocholate (mmol L^{-1})	0.08	3.00	10
Phospholipids (mmol L^{-1})	0.02	0.75	—
Lecithin (mmol L^{-1})	—	—	2
Glycerol monooleate (mmol L^{-1})	—	—	5
Sodium oleate (mmol L^{-1})	—	—	0.8
HCl solution pH 1.6 (L)	1	—	—
PBS pH 6.5 (L)	—	1	—
Maleate buffer (L)	—	—	1
Osmolarity (mOsm kg^{-1})	120	270	387
Buffer capacity (mM L^{-1} pH^{-1})	Unbuffered	10	25

Dimethylsulfoxide (DMSO), dichloromethane (DCM), methanol (MeOH), sodium chloride (NaCl), sodium hydroxide (NaOH), hydrochloric acid (HCl), and glacial acetic acid (CH_3COOH) were purchased from Fisher Chemical (Fair Lawn, NJ). Sodium phosphate monobasic anhydrous (NaH_2PO_4) and maleic acid ($C_4H_4O_4$) were purchased from Acros Organics (Geel, Belgium). *ortho*-Phosphoric acid 85% (H_3POH_4, Switzerland) was obtained from Merck, while sodium acetate anhydrous (CH_3COONa) was purchased from Macron Fine Chemicals (Center Valley, PA). Biorelevant simulated gastric and intestinal fluids, including FaSSIF/FaSSGF, and FeSSIF-V2 were purchased from Biorelevant (London, UK).

2.2. Methods

2.2.1. Dissolution media preparation. The HCl solution (pH 1.6) was prepared by dissolving 2 g of NaCl and adding 1.4 mL of concentrated HCl into water. Phosphate-buffered saline (PBS) at pH 3.0 was prepared using 7.16 g of NaCl, 3.84 g of NaH_2PO_4, and 320 μL of *ortho*-phosphoric acid (H_3PO_4), whereas PBS at pH 6.5 was prepared using 0.42 g of NaOH pellets, 3.44 g of NaH_2PO_4, and 6.19 g of NaCl. Concentrated PBS at pH 7.3 was prepared using 17.40 g of NaOH, 11.10 g of NaCl, and 68.69 g of NaH_2PO_4. Acetate buffer at pH 4.5 was prepared by dissolving 2.99 g of CH_3COONa in water along with 1.60 mL of CH_3COOH,[37] whereas acetate buffer at pH 5.0 was prepared using 13.85 g of NaCl, 2.44 g of CH_3COONa, and 980 μL of CH_3COOH in water. Maleate buffer at pH 5.8 was prepared using 6.39 g of maleic acid, 3.27 g of NaOH, and 7.33 g of NaCl. The chemicals for each buffer were solubilized in 900 mL of ultrapure water and had their pHs adjusted using either 1 mol L^{-1} NaOH or concentrated HCl solution. The volumes were then made up to 1 L with ultrapure water.

For the fasted-state simulated media preparations, 0.06 g of Biorelevant 3F powder was added in 900 mL of the prepared HCl solution at pH 1.6, while 2.24 g was dissolved in 900 mL of PBS at pH 6.5 to produce FaSSGF and FaSSIF, respectively. The fed-state simulated medium was prepared by adding 9.60 g of Biorelevant FeSSIF-V2 powder to 900 mL of maleate buffer at pH 5.8. The SIF powder was solubilized, and the volume was made up to 1 L with the appropriate buffer. For two-stage experiments in biorelevant media, Biorelevant 3F powder was added to a concentrated PBS at pH 7.3 to obtain FaSSIF at a concentration 10 times higher than required by the Biorelevant media protocol. Biorelevant media were equilibrated for 2 hours before use and were used within 48 h. Table 1 shows the composition of fasted- and fed-state simulated GI media.

2.2.2. ASDs *via* solvent evaporation (SE). ASDs of (*R*,*S*)-PZQ and (*R*)-PZQ with HPMCAS-MF and HPMC E5 LV were prepared by SE using a Hei-VAP Core rotary evaporator (Heidolph Instruments, Schwabach, Germany) equipped with an EcoChyll S Cooler (Ecodyst, Apex, NC) and a water bath set to 50 °C. The drug and polymer were dissolved in a DCM and MeOH mixture (1 : 1 v/v) to prepare ASDs with DL of 30% for (*R*,*S*)-PZQ and (*R*)-PZQ. The ASDs were subjected to further drying overnight in a vacuum oven at room temperature to remove residual solvents. A 6750 Freezer/Mill cryogenic impact mill (SPEX SamplePrep, Metuchen, NJ) was used to pulverize ASDs, and the powders were passed through a 60 mesh (250 μm) sieve to obtain a uniform particle size.

2.2.3. ASDs *via* hot-melt extrusion. HME ASDs of (*R*,*S*)-PZQ, (*R*)-PZQ with HPMCAS-MF at DL of 30% were prepared using an Xplore PME extruder (Geleen, The Netherlands) equipped with a 5 mL volume barrel set and conveying screws. A temperature of 120 ± 1 °C was used for (*R*)-PZQ ASD, while 150 ± 1 °C was used for (*R*,*S*)-PZQ ASD, with a screw speed of 20 rpm for extrudate preparation in a continuous process. All extrudates were cryomilled and passed through a 60 mesh (250 μm) sieve to obtain a uniform particle size.

2.2.4. X-ray powder diffraction. The crystallinity of starting materials ((*R*,*S*)-PZQ, (*R*)-PZQ, and polymers) and the ASDs prepared by SE and HME was assessed using a Rigaku SmartLab diffractometer (Rigaku Americas, The Woodlands, TX) equipped with a Cu Kα radiation source and D/tex ultradetector. Samples were added to glass sample holders, and X-ray powder diffraction (XRPD) patterns were recorded over the range of 4–40° 2θ at a scanning speed of 0.2 per min and a 0.02° step size with the voltage and current set to 40 kV and 44 mA, respectively.

2.2.5. Polarized light microscope (PLM). Drug crystallization was evaluated using a PLM Nikon Eclipse E600 microscope coupled to a Nikon DS-Ri2 camera (Melville, NY). Aliquots of solutions were collected during release studies and added to a slide with a concave depression (Fisher Scientific, Pittsburgh, PA). The cover glass (22 mm × 22 mm) was placed in contact with the solution, and drug crystallization was visualized under PLM using a 20× objective after sample collection. PLM images were collected using Nikon imaging software NIS Elements version 4.30.10.

2.2.6. Amorphous solubility determination. The amorphous solubility of (*R*,*S*)-PZQ and (*R*)-PZQ in different media was determined under constant stirring (400 rpm) at 37 °C using the UV-extinction method.[39] 50 mL of each aqueous medium was added to a water-jacketed beaker and allowed to equilibrate at the target temperature. Stock solutions of (*R*,*S*)-PZQ and (*R*)-PZQ in DMSO with a concentration of 125 mg mL^{-1} were added to the aqueous media at a rate of 50–200 μL min^{-1} using a syringe pump (Harvard Apparatus, Holliston, MA). Light scattering in the solution was monitored at a non-absorbing wavelength (400 nm) with a SI Photonics UV/vis spectrometer (Tucson, Arizona). A 1 mm probe was used, and data was collected at intervals of 5–10 s. The amorphous solubility of (*R*,*S*)-PZQ and (*R*)-PZQ was taken as the concentration at which a rapid increase in the amount of scattered light was observed.

2.2.7. Crystalline solubility determination. The equilibrium solubility of crystalline (*R*,*S*)-PZQ and (*R*)-PZQ was determined at 37 °C with stirring speed of 300 rpm. After 48 h, excess powder was removed by ultracentrifugation at 40 000 rpm (37 °C, 15 minutes) using an Optima L-100 XP ultracentrifuge (SW 41Ti rotor) (Beckman Coulter, Inc., Brea, CA). The supernatant was diluted in acetonitrile and water (60 : 40 v/v) and 10 μL was injected into an Agilent high-performance

liquid chromatography (HPLC) 1260 Infinity Series (Agilent Technologies, Santa Clara, CA), equipped with a G4225A HiP degasser, quaternary pump G1311B 1260 Quat Pump, an automatic sampler G1329B 1260 ALS, column compartment G1316A 1260 TCC, and UV-Vis detector G1314F 1260 VWD. An Eclipse plus C18 column (4.6 × 150 mm, 5 μm) was used with a mobile phase comprising acetonitrile and water (60 : 40 v/v) at a flow rate of 1 mL min^{-1}, an injection volume of 10 μL, and an ultraviolet (UV) detector set at 220 nm. Data were collected and processed using OpenLab CDS ChemStation Edition, Rev. C.01.05. A stock solution of (*R*,*S*)-PZQ at 20 mg mL^{-1} in the mobile phase was prepared, and PZQ solubility was obtained from a standard curve in the range of 1–300 μg mL^{-1}.

2.2.8. Powder release studies. Powder release studies were conducted in triplicate in single-stage or two-stage experiments using a USP II dissolution apparatus (Hanson Vision G2 Classic 6, Teledyne Hanson Research, Chatsworth, CA). An *in situ* Rainbow fiber optic ultraviolet spectrometer coupled with 2 or 5 mm fiber optic dip probes (Pion, Billerica, MA, USA) was used to monitor drug concentration over 2 h at 37 °C with 100 rpm of paddle stirring. Data were collected and treated using the AuPRO software, version 6.0.1.5775. The target PZQ concentration for release studies was either 667 μg mL^{-1} or 1.5 mg mL^{-1}, which is close to PZQ amorphous solubility.

For single-stage experiments, ASD powders of (*R*,*S*)-PZQ and (*R*)-PZQ were added to 50 mL of PBS at pH 6.5, FaSSIF, or FeSSIF-V2. The two-stage release experiments were performed under gastric conditions at pH 1.6, 3.0, or 5.0, for 1 h, then shifted to pH 6.5 for an additional hour. The drug release was conducted in 45 mL of gastric fluid at pH 1.6, followed by the addition of 5 mL of concentrated PBS pH 7.3 to adjust the pH of the solution to pH 6.5. Release studies in media at pH 3.0 and pH 5.0 were conducted in 47 mL and 48 mL, respectively, and after 1 h, volumes were made up to 50 mL with concentrated PBS at pH 7.3. The fasted-state two-stage experiments were performed in 45 mL of FaSSGF (pH 1.6), followed by the addition of 5 mL of 10× concentrated FaSSIF solution (0.57 mol L PBS, pH 7.3) to achieve 50 mL of FaSSIF pH 6.5. The fed-state condition was performed in 45 mL of acetate buffer pH 4.5, followed by the addition of 5 mL of 10× concentrated FeSSIF-V2 (pH 12) to achieve 50 mL FeSSIF-V2 pH 5.8.

A 5 mm fiber optic dip probe was used to monitor drug concentration in aqueous and fasted-state media, and for fed-state media, a 2 mm fiber optic dip probe was required. Second derivative analysis was applied to correct the spectral baseline, and a calibration curve of the area under the curve (AUC) for the range 278–285 nm was used to calculate the drug concentration in all media, except for FeSSIV-V2, for which a second derivative analysis at 280 nm was employed. Calibration curves in solutions at pH 1.6, 4.5, 6.5, FaSSGF, FaSSIF, and FeSSIF-V2 were built over the concentration range of 10–1500 μg mL^{-1}, while those at pH 3.0 and 5.0 ranged from 10–1400 μg mL^{-1}.

2.2.9. Differential scanning calorimetry (DSC) analysis. The melting peak temperature (T_m) and midpoint glass transition temperature (T_g) of (*R*,*S*)-PZQ and (*R*)-PZQ raw materials were determined using a TA Instruments Discovery DSC 2500 equipped with an RCS90 refrigerated cooling accessory (TA Instruments, New Castle, DE). Measurements were conducted under a dry nitrogen atmosphere at a flow rate of 50 mL min^{-1}. Temperature calibration was performed with indium and n-octadecane, while enthalpy and heat capacity calibrations were conducted using indium and sapphire disks. Approximately 1 mg of each sample was sealed in Tzero aluminum pans (TA Instruments) and equilibrated at 20 °C. The samples were then heated at 10 °C min^{-1} to 150 °C for (*R*,*S*)-PZQ and 120 °C for (*R*)-PZQ, held isothermally for 3 minutes, cooled to −75 °C at 20 °C min^{-1}, and subsequently reheated at 10 °C min^{-1} to just above the respective melting points.

2.2.10. Statistical analysis. Microsoft Excel 365 (Microsoft Corporation, Redmond, WA, USA) was used to apply the *F*-test and unpaired *t*-test on solubility results.

3. Results

3.1. Amorphous and crystalline solubility of PZQ

Table 2 presents the amorphous and crystalline solubilities of PZQ in aqueous media with different pH values and in fasted- and fed-state simulated media. The solubility of crystalline

Table 2 Amorphous and crystalline solubility of PZQ

	Amorphous solubility (mg mL^{-1})		Crystalline solubility (mg mL^{-1})			
Medium	(*R*,*S*)-PZQ	(*R*)-PZQ	(*R*,*S*)-PZQ	(*R*)-PZQ	(*R*,*S*)-PZQ A/C[a]	(*R*)-PZQ A/C[a]
pH 1.6	1.41 ± 0.02	1.40 ± 0.02	0.19 ± 0.01	0.27 ± 0.00	7.4	5.2
pH 3.0	1.26 ± 0.02	1.26 ± 0.01	0.17 ± 0.00	0.23 ± 0.02	7.6	5.5
pH 4.5	1.43 ± 0.01	1.35 ± 0.04	0.21 ± 0.01	0.29 ± 0.01	6.8	4.7
pH 5.0	1.23 ± 0.02	1.20 ± 0.01	0.16 ± 0.01	0.24 ± 0.01	7.7	5.0
pH 5.8	1.30 ± 0.09	1.33 ± 0.01	0.18 ± 0.00	0.27 ± 0.00	7.2	4.9
pH 6.5	1.17 ± 0.05	1.39 ± 0.05	0.17 ± 0.01	0.27 ± 0.01	6.9	5.1
FaSSGF	1.55 ± 0.02	1.63 ± 0.04	0.22 ± 0.01	0.28 ± 0.00	7.0	5.8
FaSSIF	1.49 ± 0.11	1.67 ± 0.04	0.22 ± 0.01	0.32 ± 0.01	6.8	5.2
FeSSIF-V2	1.74 ± 0.09	1.70 ± 0.10	0.31 ± 0.01	0.43 ± 0.00	5.6	4.0

[a] Ratio between amorphous and crystalline PZQ solubility.

PZQ in different media at 37 °C ranged from 0.17 to 0.31 mg mL^{-1} for (*R*,*S*)-PZQ, and from 0.23 to 0.43 mg mL^{-1} for (*R*)-PZQ. The corresponding amorphous solubility for (*R*,*S*)-PZQ ranged from 1.17 to 1.54 mg mL^{-1}, while that of (*R*)-PZQ ranged from 1.20 to 1.67 mg mL^{-1}. The PZQ solubilities are in line with the previously reported values for racemic and enantiopure PZQ in aqueous media.[28,40,41] Solubility was found to be independent of pH, consistent with the molecular structure. Furthermore, solubilization by micellar species present in biorelevant media was low. Finally, little difference was noted between the amorphous solubility values for (*R*,*S*)-PZQ *versus* (*R*)-PZQ, while the crystalline form of (*R*)-PZQ showed a slightly higher solubility than (*R*,*S*)-PZQ.

3.2. Powder release studies of PZQ-ASDs

The influence of pH and fasted/fed-state simulated media on drug release from ASD powders manufactured by SE or HME, containing enantiopure *versus* racemic PZQ and formulated with HPMCAS MF or HPMC E5 LV, was evaluated. These polymers have demonstrated promising drug release and stability at a DL of 30% in previous studies,[42] and hence were evaluated further.

3.2.1. Release studies in aqueous media. At a PZQ target concentration of 667 μg mL^{-1}, HPMCAS-based ASDs presented a similar drug release profile in single-stage experiments in PBS pH 6.5 (Fig. 2A), independent of if the ASD comprised the racemate or enantiomer. The (*R*,*S*)-PZQ-HPMCAS HME and (*R*)-PZQ-HPMCAS SE formulations showed complete release at approximately 40 minutes, while (*R*,*S*)-PZQ-HPMCAS SE had a slightly slower dissolution rate, releasing 91% at the same dissolution time and achieving complete release within 100 minutes. In the two-stage experiments (Fig. 2B), formulations with HPMCAS-based ASDs presented poor drug release (no more than 30%) over the first hour of dissolution due to the low solubility of HPMCAS MF in solutions with a pH lower than ~6.0.[43,44] However, after shifting the pH to 6.5, HPMCAS-based ASDs achieved drug release higher than 92% within 120 minutes.

At a PZQ target concentration of 1.5 mg mL^{-1}, (*R*,*S*)-PZQ-HPMCAS prepared by different processing methods showed a similar release profile in PBS pH 6.5 (single-stage), reaching 78% and 71% for the HME and SE methods, respectively (Fig. 2C). Additionally, (*R*)-PZQ-HPMCAS SE showed a higher dissolution rate than (*R*)-PZQ-HPMCAS HME, but by the end of the experimental time frame, both samples achieved a drug release of approximately 88%. As observed at the low target concentration, the HPMCAS-based ASD released poorly in pH 1.6 medium (Fig. 2D). After shifting to pH 6.5, the drug release of (*R*,*S*)-PZQ-HPMCAS peaked at 73% and 69% for samples obtained by SE and HME methods, respectively, while the (*R*)-PZQ-HPMCAS SE drug release achieved 91%.

For the ASD formulations containing HPMC, the (*R*,*S*)-PZQ-HPMC SE sample reached a drug release of 82% at the end of the single-stage experiments at a concentration of 667 μg mL^{-1} (Fig. 2A). The same formulation showed a drug release of 96% at 68 minutes and the concentration level remained stable at intestinal pH (Fig. 2B). The ASD composed of (*R*)-PZQ with HPMC E5 LV presented a maximum drug release of 86% (~25 min) and 99% (~49 min) in the single-stage and two-stage experiments, respectively. Subsequently, these samples experienced a slight drop of 1% in drug concentration after 120 minutes, likely due to drug crystallization.

The (*R*,*S*)-PZQ-HPMC SE sample released 55% at 39 min and increased slowly to 65% in the single-stage experiment at a target concentration of 1.5 mg mL^{-1}. In contrast, (*R*)-PZQ-HPMC SE showed a drug release of 65% at the same time, and afterwards, dropped to 60% over the experimental time frame period (Fig. 2C). In the two-stage experiments (Fig. 2D), HPMC-based ASDs exhibited similar drug release extent, with the formulation containing the PZQ racemate releasing slower (71% at 60 minutes) than the enantiopure form (71% at

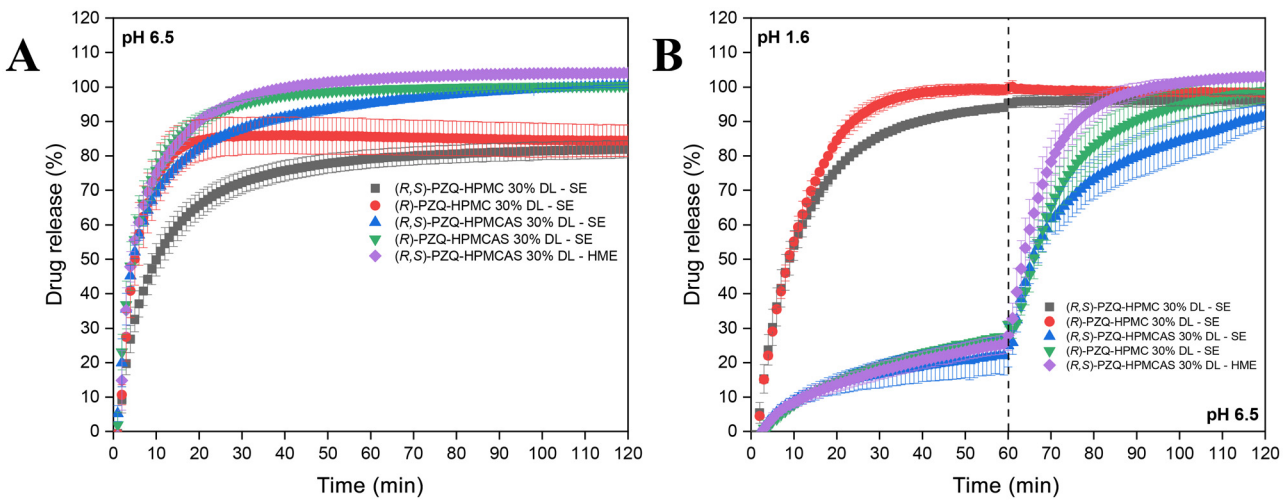

Fig. 2 Single- and two-stage release experiments with PZQ ASD samples prepared by SE and HME in aqueous media. PZQ target concentrations: 0.667 mg mL^{-1} for A and B; 1.5 mg mL^{-1} for C and D.

26 minutes). After reaching maximum release, (*R*,*S*)-PZQ-HPMC SE remained almost constant over the dissolution experiment, whereas (*R*)-PZQ-HPMC SE concentration decreased.

Two-stage experiments were also carried out with media at pH 3.0 or pH 5.0, followed by a shift to pH 6.5. The HPMCAS-based ASDs did not exceed a drug release of 25% in the first dissolution state (gastric pH), but the release increased after shifting to intestinal pH. The samples prepared with HPMCAS presented similar drug release profiles and ranged from 62% to 77% in dissolution experiments at low target concentration (Fig. S1A and S1B†), and from 43% to 58% at high target concentration (Fig. S1C and S1D†). At low PZQ target concentration, HPMC-based ASDs showed very similar drug release profiles, with a drug release higher than 85% up to 35 min, which remained steady over the intestinal pH (Fig. S1A and S1B†). On the other hand, at high target concentration, HPMC-based ASDs released slightly faster in pH 5.0 than in pH 3.0. For (*R*)-PZQ-HPMC SE, a maximum drug release of 72% was observed at pH 5.0 and 68% at pH 3.0, and subsequently, the drug concentration decreased in both experiments (Fig. S1C and S1D†) due to PZQ crystallization.

3.2.2. Release studies in fasted-state simulated media. The ASD samples studied exhibited complete or nearly complete release in approximately 30 minutes whereby the concentration remained constant over the experimental time frame in FaSSIF, when dosed at a concentration of 0.667 μg mL^{-1}, as shown in Fig. 3A. Compared to single-stage experiments in PBS pH 6.5, no relevant differences were observed for ASD samples in FaSSIF, except that HPMC-based ASDs showed a slight improvement in drug release. For two-stage experiments, HPMCAS-based ASDs released PZQ poorly in FaSSGF, but complete or nearly complete release was observed in FaSSIF at both low and high target concentrations. In the single-stage experiment at high target concentration, HPMCAS-based ASDs released more than 85% of the drug within 60 minutes, while more than ~90% release was observed in two-stage experiments (Fig. 3B–D).

HPMC-based ASDs achieved 93% (~25 min) in FaSSIF and complete drug release in simulated gastric media at low target concentration (Fig. 3A and B). (*R*,*S*)-PZQ-HPMC and (*R*)-PZQ-HPMC reached respectively 82% (~40 minutes) and 75% (~19 minutes) at a high target concentration in the simulated intestinal fluid, and then exhibited a 30% drop in release (Fig. 3C). A decrease in the release was also observed after reaching ~75% release for formulations with HPMC in the two-stage experiments (Fig. 3D). The drop in release reflects a concentration decreased resulting from PZQ crystallization. HPMC has been demonstrated to be less effective in drug stabilization against crystallization than either HPMCAS MF or LF grades.[42] The ASD samples had an increase in the drug release in FaSSIF medium compared to in PBS pH 6.5 medium at high target concentration, which was more evident with samples prepared with the racemic form of PZQ and HPMCAS. This increase in drug release is likely due to the slightly enhanced solubility of the drug in the FaSSIF medium (Table 2). Bile salts present in the medium can improve drug solubility through micellar incorporation, improving the dissolution rate.[45–47] However, this effect is relatively minor for PZQ.

3.2.3. Release studies in fed-state simulated media. ASD samples in FeSSIF-V2 single-stage experiments showed a release of approximately 70–80% at a concentration of 0.667 mg mL^{-1}, while no more than 55% release was observed at 1.5 mg mL^{-1}. As expected in two-stage experiments, HPMCAS-based ASDs exhibited low drug release in simulated gastric medium (pH 4.5), but a drug release of approximately 64% and 32% was observed in FeSSIF-V2 at low and high target concentration, respectively for the second stage (Fig. 4A–D).

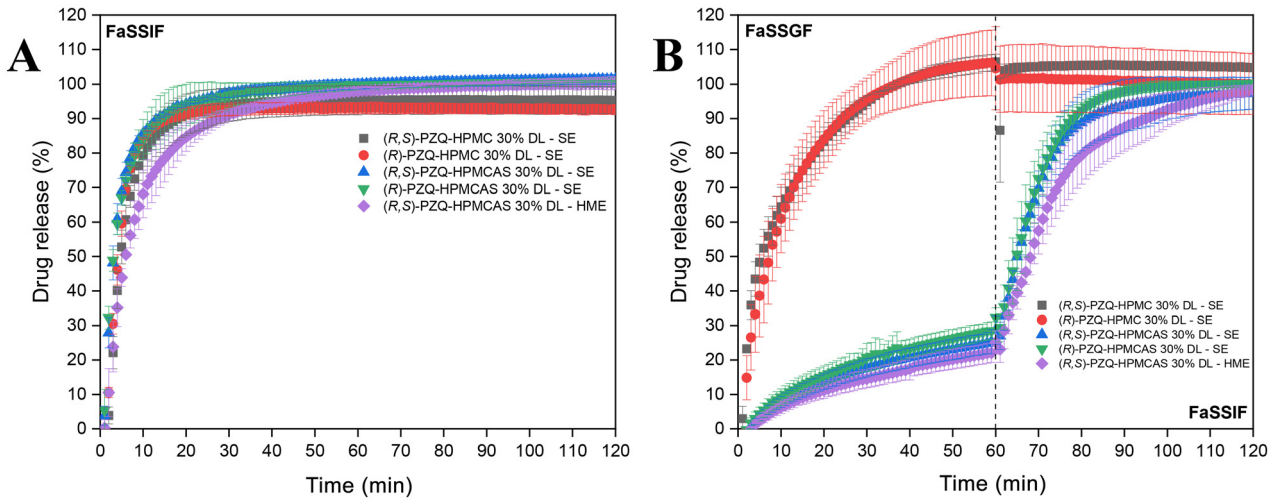

Fig. 3 Single- and two-stage release experiments in fasted-state simulated media with PZQ ASD samples prepared by SE and HME. PZQ target concentrations: 0.667 mg mL^{-1} for A and B; 1.5 mg mL^{-1} for C and D.

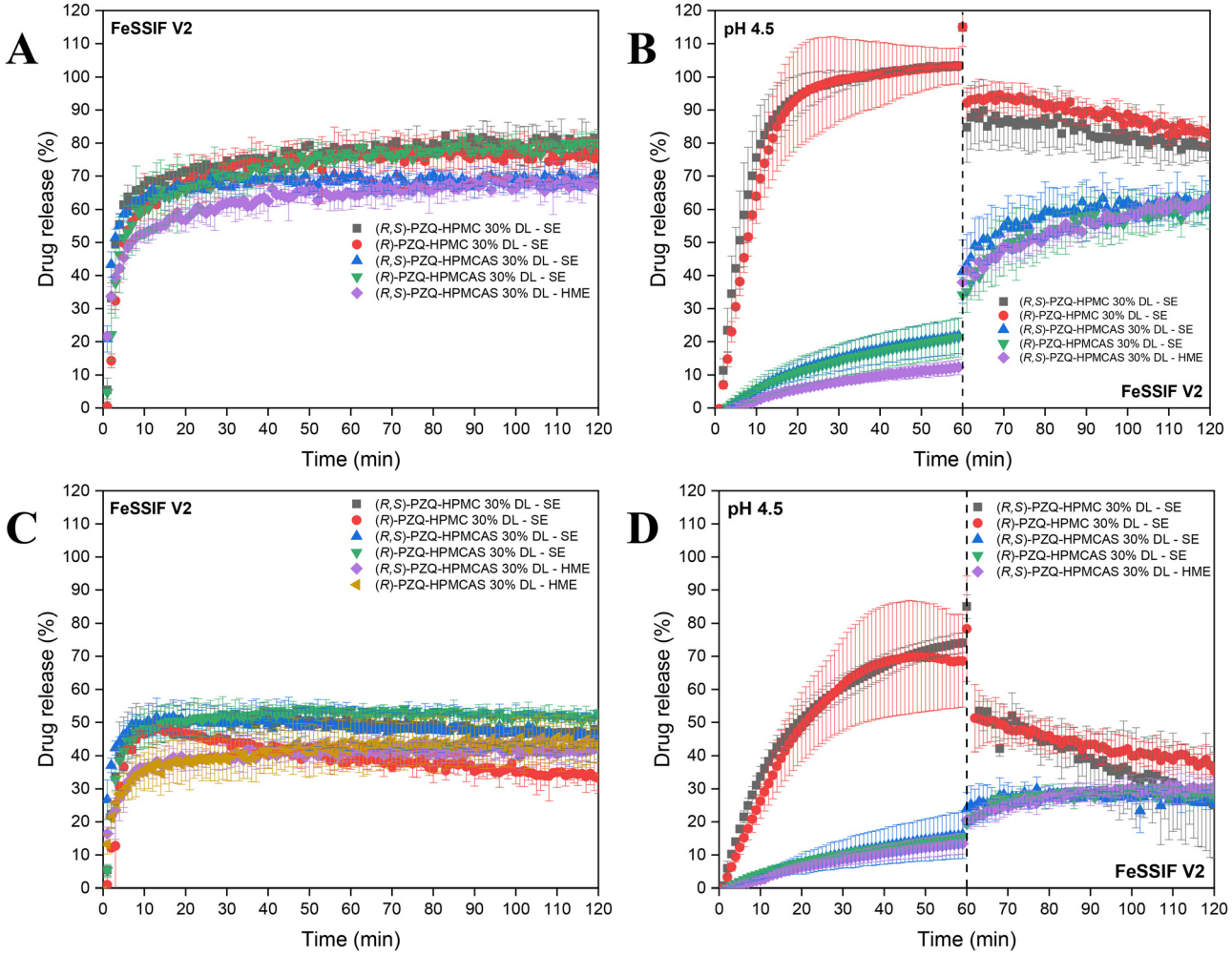

Fig. 4 Single- and two-stage release experiments in fed-state simulated media with PZQ ASD samples prepared by SE and HME. PZQ target concentrations: 0.667 mg mL^{-1} for A and B; 1.5 mg mL^{-1} for C and D.

HPMC-based ASDs presented complete release (~35 minutes) at pH 4.5 and 70% release at low and high target concentration, respectively. Upon shifting to FeSSIF-V2 medium, a decrease in drug release was observed for HPMC-based ASDs, which may be related to drug crystallization.

3.3. PLM analysis

PLM images were collected during release studies at 5, 60, and 120 minutes to evaluate the presence of crystals at a PZQ target concentration of 1.5 mg mL^{-1}. PLM images showed particles with no evidence of birefringence for HPMCAS-based ASDs in all instances (Fig. S2–S7†). Even in experiments performed in fed-state simulated media using a two-stage dissolution approach, where drug release was less than 32%, no evidence of PZQ crystallization in HPMCAS-based ASDs was observed using PLM. Thus, the particles appear to consist of undissolved ASD.

Birefringence was clearly observed in both the racemic and enantiopure forms of PZQ with HPMC E5 LV after 60 min (Fig. 5, S8, and S9†). Birefringent particles with needle-like and rectangular morphologies were observed for (*R*)-PZQ-HPMC SE and (*R*,*S*)-PZQ-HPMC SE samples, respectively. Since HPMC-based ASDs already presented evidence of crystallization in both single-stage and two-stage experiments in aqueous media, PLM images were not collected from these samples in FaSSGF or FaSSIF.

In fed-state simulated media, HPMC-based ASDs showed no presence of crystals in acetate buffer pH 4.5, but crystallization was observed at the beginning of dissolution in the single-stage experiments and after shifting to FeSSIF-V2 medium (Fig. 6 and S10†).

3.4. PXRD analysis

3.4.1. PXRD analysis of PZQ-ASD samples. ASDs prepared with (*R*,*S*)-PZQ and (*R*)-PZQ by SE and HME were analyzed by PXRD to evaluate residual crystallinity. The diffractogram profiles were compared to the neat forms of PZQ or polymer, as well as the physical mixture of PZQ and polymer. Diffractograms of PZQ ASDs did not show any sharp peaks,

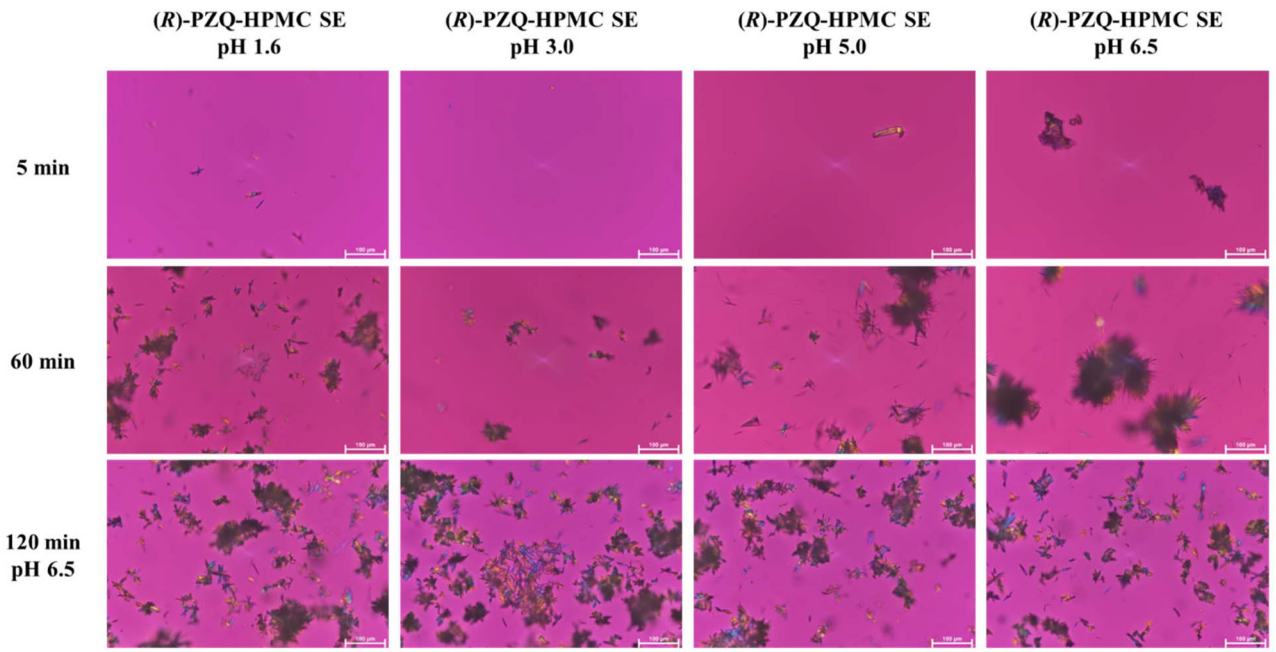

Fig. 5 PLM images of (*R*)-PZQ-HPMC ASD obtained during the release studies in aqueous media.

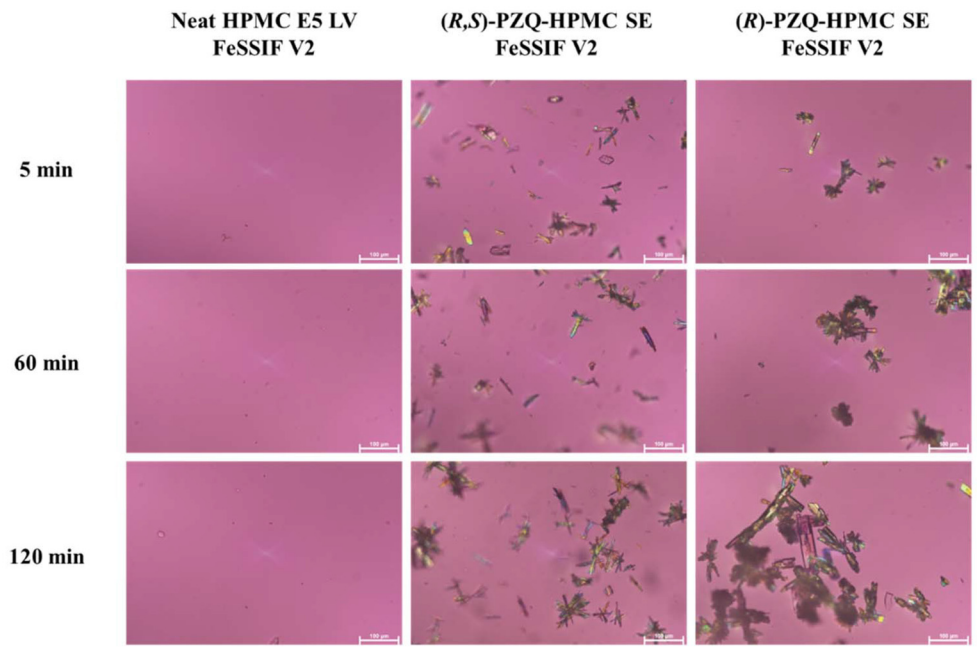

Fig. 6 PLM images of neat HPMC E5 LV, (*R*,*S*)-PZQ-HPMC SE, and (*R*)-PZQ-HPMC SE obtained during the release studies in fed-state simulated media.

confirming that the samples were in an X-ray amorphous state after preparation by either SE or HME (Fig. S11†).

3.4.2. PXRD analysis after release studies. After release studies, solutions were filtered using a 0.45 μm filter to collect the residue, which were then analyzed by PXRD to verify the presence of crystals. Fig. 7 shows diffractograms for samples obtained after release studies. Both racemic and enantiopure forms of PZQ formulated with HPMC E5 LV *via* SE presented crystalline peaks in aqueous media after single and two-stage experiments.

The (*R*,*S*)-PZQ-HPMC ASD sample exhibited small peaks at 7.8°, 15.0°, 19.8°, and 25.2° 2θ, characteristic of crystalline (*R*, *S*)-PZQ (Fig. 7A). Samples from release studies with a pH switch from 5.0 to 6.5 presented a small peak at 31.5°, attribu-

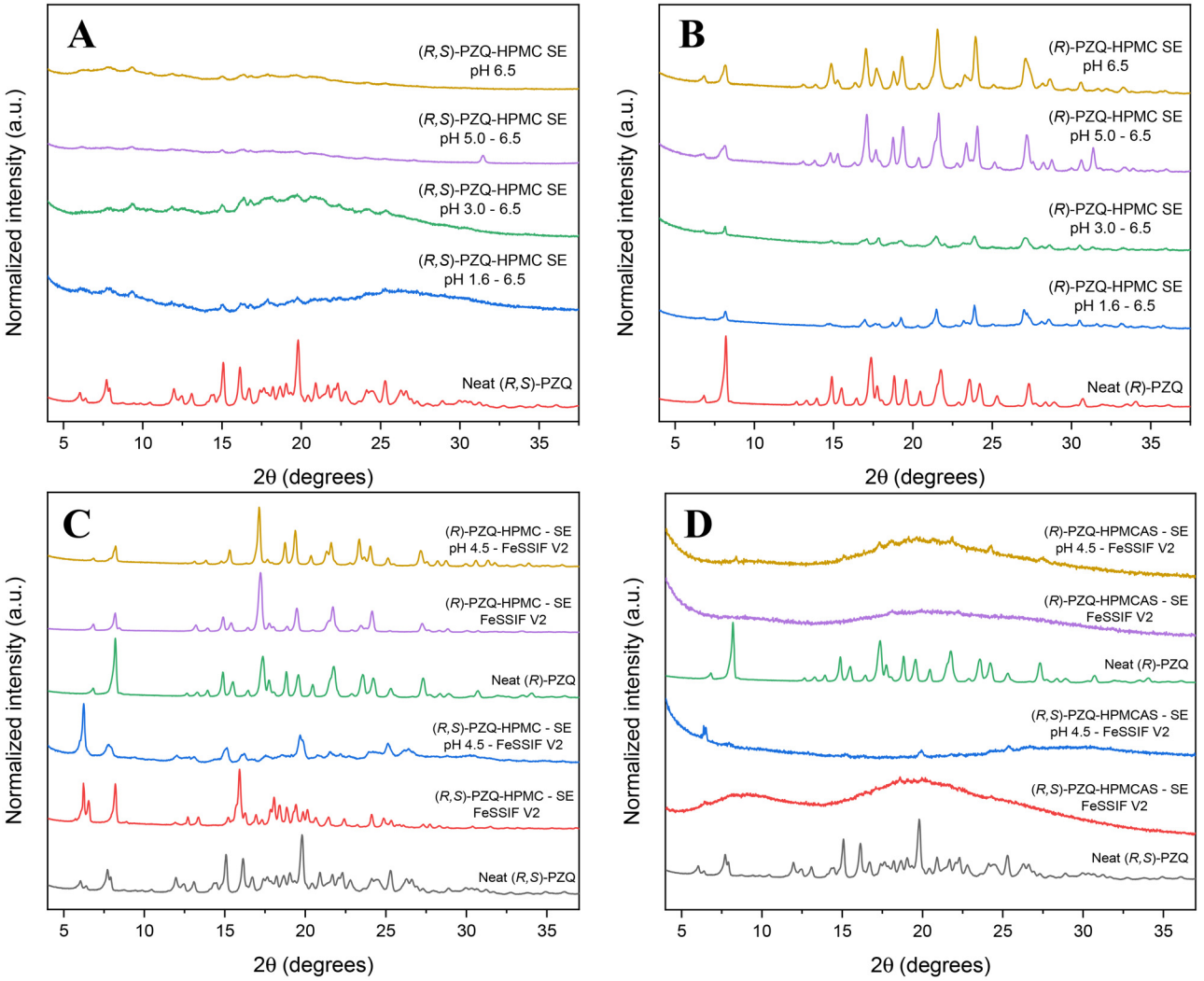

Fig. 7 Diffractograms of neat PZQ and PZQ ASDs prepared by solvent evaporation after release studies in single and two-stages experiments. (A) (*R,S*)-PZQ-HPMC and (B) (*R*)-PZQ-HPMC in aqueous media, (C) PZQ-ASDs formulated with HPMC, and (D) PZQ-ASDs with HPMCAS in fed-state simulated media.

ted to NaOH. The (*R*)-PZQ-HPMC SE ASD presented characteristic peaks of the neat crystalline (*R*)-PZQ at 8.3°, 14.9°, 17.4°, 19.6°, 21.8°, 24.3°, and 27.3° 2*θ* (Fig. 7B). Some peaks were slightly shifted due to sample non-uniformity in the aluminum cavity holder. Since PXRD was utilized solely for qualitative analysis, the variations in signal intensities of (*R*)-PZQ-HPMC and (*R,S*)-PZQ-HPMC SE should not be attributed only to crystalline concentration in the sample. Additionally, factors such as crystal size and degree of crystalline ordering, as well as sample mass also affect signal intensity.

Formulations prepared with racemic and enantiopure forms of PZQ presented crystalline peaks with either HPMC or HPMCAS in fed-state simulated media in both single and two-stage experiments (Fig. 7C, D, and S12†). The peaks were more intense for HPMC ASDs, while they were much smaller for HPMCAS-based ASDs. ASD formulations containing HPMCAS with (*R,S*)-PZQ or (*R*)-PZQ in aqueous media or fasted-state simulated media were not analyzed by PXRD, since these samples showed no evidence of crystallinity in PLM images or a decrease in drug release during the dissolution experiments.

4. Discussion

4.1. Crystalline and amorphous solubility of PZQ

The solubility of PZQ was determined in aqueous media across various pH levels, as well as in fasted- and fed-state simulated GI media. The amorphous solubility of (*R,S*)-PZQ and (*R*)-PZQ was approximately 8- and 6-fold greater than in the corresponding crystalline state. According to the *t*-test, there is no statistically significant difference in amorphous solubility at the 95% confidence level between the racemic and enantiopure forms of praziquantel (PZQ) across different media,

except in PBS pH 6.5, where a significant difference was observed in the amorphous solubility.

The amorphous and crystalline solubilities of PZQ exhibited minimal variation in aqueous media. This result is consistent with the calculated pK_a of 1.14 (Fig. S13†),[48] which suggests limited ionization-dependent solubility changes across the studied pH range. The solubility of PZQ in both amorphous and crystalline forms exhibited higher values in FeSSIF-V2, probably due to the higher concentration of bile salts (10 mmol L^{-1} sodium taurocholate) present in this medium. However, the solubility enhancement observed in FeSSIF-V2 was modest which suggests that PZQ has limited interaction with micellar components. Interestingly, it has been reported that both high fat and high carbohydrate diets increase the bioavailability of praziquantel, with a high carbohydrate diet resulting in a greater increase.[49] Thus, the positive food effect could depend on factors other than an increase in drug solubility which is quite moderate in FeSSIF-V2.

4.2. Impact of polymer type on drug release

ASD formulations can enhance drug solubility leading to supersaturated solutions upon dissolution, resulting in higher membrane flux and improved absorption and bioavailability. The polymer used to form the ASD, serving an important role in maintaining drug supersaturation by preventing both nucleation and crystal growth – processes involved in crystallization.[50,51] HPMCAS and HPMC have been widely employed as drug crystallization inhibitors.[52,53] Furthermore, a previous study has demonstrated that they are able to delay crystallization of PZQ,[42] motivating the studies performed herein.

The influence of the polymer on PZQ release was evaluated in ASD samples composed of HPMCAS MF or HPMC E5 LV with (*R*,*S*)-PZQ and (*R*)-PZQ prepared *via* SE. ASD samples prepared with HPMC E5 LV showed a greater extent of drug release in the first dissolution stage than those prepared with HPMCAS MF in experiments initiated at pH 1.6, 3.0, 4.5, 5.0, fasted- and fed-state simulated media (two-stage) (Fig. 2–4, and S1†). (*R*)-PZQ-HPMC SE showed a decrease in drug release with time in all dissolution media studied at a high PZQ dose concentration, and (*R*,*S*)-PZQ-HPMC SE had a decrease in drug release with time only in the fasted- and fed-state simulated media (Fig. 3 and 4). These observations indicate that (*R*)-PZQ has a higher tendency to crystallize from highly supersaturated solutions than the racemic form. This observation is consistent with a previous study that found that (*R*)-PZQ had a shorter nucleation induction time than the racemic form, from supersaturated solutions.[42] The release results further demonstrated that HPMC E5 LV was not sufficiently effective in preventing PZQ crystallization during dissolution, as confirmed by PLM and PXRD (Fig. 5 and S9†). ASD samples with HPMC E5 LV (approximately 70%) showed little difference in the extent of release for different pH conditions. On the other hand, formulations containing HPMCAS MF did not show a decrease in drug concentration with time, except in fed-state simulated media, consistent with HPMCAS MF being a better nucleation inhibitor.[47,54,55] XRD analysis revealed that formulations containing HPMCAS exhibited drug crystallization in FeSSIF-V2. Thus, the higher concentration of bile salts and lecithin present in FeSSIF-V2 promoted crystallization, which could not be as effectively inhibited by HPMCAS when compared to buffer. A previous study with the poorly soluble compounds, posaconazole and atazanavir, found that induction times were much longer in buffer than in FaSSIF when HPMCAS was present in both instances.[56] In other words, the crystallization inhibitory power of a polymer was diminished when bile salts and lecithin were present. Therefore, the increased crystallization tendency following (*R*,*S*)-PZQ and (*R*)-PZQ ASD dissolution in FeSSIF-V2 is in broad agreement with these previous observations.

HPMCAS-based ASDs released poorly at low pH, but had similar or greater release than HPMC E5 LV ASDs after 2 h in PBS pH 6.5 (single stage), pH-shift experiment from pH 1.6 to pH 6.5 fasted state media, and in FeSSIF-V2 (single stage). HPMCAS has pH-dependent solubility and is insoluble at gastric pH due to the minimal ionization of succinoyl groups, explaining why ASD samples with this polymer showed limited dissolution at low pH, with drug release below 30%. This aligns with its resistance to gastric dissolution and its role as an enteric polymer, solubilizing in media with pH ~ 5.5–6.

No decrease in drug release with time was observed with HPMCAS-based ASDs, suggesting that HPMCAS MF better inhibits crystallization from supersaturated PZQ solutions than HPMC E5 LV. It is worth noting that neither polymers could prevent PZQ crystallization in FeSSIF-V2, as observed through PLM and PXRD analyses, although the extent of crystallization was much smaller for HPMCAS formulations (Fig. 7). Samples formulated with HPMC E5 LV showed nearly immediate PZQ crystallization in FeSSIF-V2 (Fig. 6 and S10†), which could be related to the rapid decrease in drug release extent during the transition to FeSSIF-V2 in the two-stage experiments. Further studies are needed to understand the stability of supersaturated PZQ solutions in fed-state simulated media.

4.3. Impact of chirality on drug release

The therapeutic efficacy of PZQ is attributed mostly to (*R*)-PZQ while the (*S*) enantiomer and its metabolites do not contribute to the therapeutic effect, but does lead to side effects and a bitter taste.[57] A formulation produced with only (*R*)-PZQ is expected to eliminate most of the drawbacks of the racemic form, and would further allow the tablet size/overall dose to be reduced by half. Given this, the exclusion of (*S*)-PZQ is crucial to improve dosing of PZQ. In this work, (*R*)-PZQ-ASDs were evaluated to determine whether they could provide better performance and serve as an alternative to the commercially available racemic crystalline PZQ mixture. If bioavailability enhancement could be achieved, as has been observed in preclinical models with racemic PZQ-ASDs,[24,27,58] the dose could be further reduced, mitigating the increased production costs of isolating the (*R*) enantiomer.

The enantiomer (*R*)-PZQ formulated with HPMC showed a similar or better dissolution rate and extent of drug release

than the corresponding ASD with (*R*,*S*)-PZQ in aqueous media at low or high target concentrations. After achieving the maximum extent of drug release, the (*R*)-PZQ-HPMC SE ASD exhibited a faster decrease in drug concentration at the high target concentration than (*R*,*S*)-PZQ-HPMC SE, particularly in pH-shift experiments from pH 3.0 or 5.0 to 6.5, in PBS pH 6.5 (single-stage) and FaSSIF (single stage). Crystals of both the enantiopure and racemic forms of PZQ formulated with HPMC were clearly observed during PLM monitoring, which was also confirmed by PXRD analysis after release studies. Notably, (*R*,*S*)-PZQ-HPMC and (*R*)-PZQ-HPMC showed a greater drug release in FaSSIF as compared to in PBS pH 6.5 at high concentration, but the presence of bile salts may have also contributed to the faster crystallization of (*R*)-PZQ. No significant difference was observed between the enantiopure and racemic mixture of PZQ formulated with either HPMCAS or HPMC in FeSSIF-V2. PZQ crystallization tendency is theoretically associated with the crystal lattice energy and solvation of components that vary for each drug solid state form and affect the crystallization kinetics.[59] Since the (*R*,*S*)-PZQ anhydrous (Form A) and (*R*)-PZQ hemihydrate were formed herein, polymers can interact differently with the drug based on its conformational structure, thereby impacting crystal growth, and the thermodynamic driving force for crystallization likely differs between racemate and enantiomer. In the enantiopure (*R*)-PZQ, all molecules have the same stereochemistry, which can lead to more efficient molecular packing and stronger intermolecular interactions. This can promote a higher nucleation rate compared to the racemic compound, where the presence of both *R*- and *S*-enantiomers leads to less favorable packing and where the counter-enantiomer can act as an "impurity".[60] The greater crystallization tendency of an enantiomer over a racemate in the amorphous form has been noted previously.[60]

The enantiopure form and racemic PZQ mixture, when formulated with HPMCAS, released drug similarly in all release conditions studied, except in PBS pH 6.5 and pH shift experiment from pH 1.6 to 6.5, where (*R*)-PZQ-HPMCAS (SE) had a better release rate and extent than (*R*,*S*)-PZQ-HPMCAS (SE). Based on the calculated pK_a of 1.14, PZQ remained predominantly as a neutral form under the conditions studied, suggesting minimal pH-dependent solubility and little-to-no ionization in low-pH conditions. Indeed, the amorphous and crystalline solubilities of (*R*,*S*)-PZQ and (*R*)-PZQ showed no substantial differences across the pH range investigated. The improved release observed for (*R*)-PZQ-HPMCAS compared to (*R*,*S*)-PZQ-HPMCAS is likely attributable to the slightly higher amorphous solubility of (*R*)-PZQ in PBS pH 6.5. This is supported by the maximum concentrations achieved during dissolution, which were approximately 1.4 mg mL^{-1} for (*R*)-PZQ-HPMCAS SE and 1.1 mg mL^{-1} for (*R*,*S*)-PZQ-HPMCAS SE, in agreement with the amorphous solubility data presented in Table 1.

4.4. Impact of processing method type on drug release

(*R*,*S*)-PZQ has good thermal stability upon reaching its melting point (T_m) of 136–142 °C,[61] but undergoes significant thermal decomposition above 200 °C.[62] (*R*)-PZQ possesses a slightly lower T_m 113–115 °C,[63] and, unless influenced by chirality-specific interactions, this enantiomer should likely follow a similar decomposition temperature to that of the racemic PZQ mixture. The glass transition temperature (T_g) of (*R*,*S*)-PZQ has been reported to be around 38 °C,[14] in good agreement with the value obtained herein (around 37 °C, Fig. S14†). The T_g of (*R*)-PZQ was observed at around 34 °C, consistent with its lower T_m. The thermal stability of PZQ makes it a promising candidate for preparation *via* HME, where the typical processing temperature exceeds the drug's melting point and is 15–60 °C higher than the polymer's glass transition temperature[64] (around 154 °C for HPMC[65] and 120 °C for HPMCAS[66]), although this latter criterion can be reduced if plasticization by the drug occurs.[67–69] Based on the T_g values of (*R*,*S*)-PZQ and (*R*)-PZQ, plasticization of both polymers would occur. Consequently, X-ray amorphous extrudates of both systems could be prepared at reasonable temperatures. Additionally, HME samples benefit from the inherent advantages of the technique, such as continuous manufacturing, solvent-free processing, potential for automation, and the possibility of real-time monitoring.[70]

To evaluate the impact of the processing method on PZQ release, (*R*,*S*)-PZQ and (*R*)-PZQ were formulated with HPMCAS MF *via* SE and HME. HPMC-based ASDs *via* SE had a higher tendency to crystallize compared to those prepared with HPMCAS under most dissolution conditions studied and, therefore, formulations with HPMC were not prepared by HME. The racemic form of PZQ prepared by both SE and HME exhibited a very similar dissolution profile, achieving an equivalent dissolution rate and extent of release in most media. Thus, the (*R*,*S*)-PZQ-HPMCAS sample was studied under all conditions, whereas (*R*)-PZQ, where material was limited, was evaluated only using single-stage experiments in PBS pH 6.5 and FeSSIF-V2 at a high target concentration.

Despite presenting a slightly slower dissolution rate in PBS pH 6.5, the (*R*)-PZQ-HPMCAS HME ASD presented the same extent of release as the formulation prepared by SE at the end of the experiment. HPMCAS-based ASDs prepared by HME released slightly less than those prepared by SE in FeSSIF-V2, which can be attributed to different extents of drug crystallization as confirmed by PXRD analysis. These results demonstrated that preparation approach for both the enantiopure and racemic forms of PZQ ASDs had no discernable impact on PZQ dissolution.

5. Conclusions

This work evaluated the impact of polymer type, processing method, and chirality on PZQ release in ASD formulations of racemic and enantiopure PZQ at a DL of 30% in simple aqueous media and under fasted/fed-state media conditions. The medium pH had no influence on PZQ drug release when formulated with HPMC E5 LV, but these formulations exhibited lower stability to crystallization than HPMCAS-based ASDs

during release studies. PZQ crystallization was observed through PLM images and PXRD analyses in HPMC-based ASDs under all release conditions. Although formulations containing HPMCAS MF released poorly at gastric pH due to low solubility of HPMCAS MF at low pH, (*R*,*S*)-PZQ-HPMCAS and (*R*)-PZQ-HPMCAS demonstrated good release in PBS pH 6.5 and fasted-state simulated media. HPMCAS-based ASDs showed no evidence of crystallization, except in fed-state simulated media, and HPMCAS was more effective as a crystallization inhibitor compared to HPMC E5 LV.

The enantiopure (*R*)-PZQ formulated with HPMCAS MF released more than (*R*,*S*)-PZQ-HPMCAS in PBS pH 6.5 at high target concentration, but both formulations had a similar performance in fasted-state simulated media due to enhanced solubility of PZQ induced by the presence of bile salts. (*R*,*S*)-PZQ-HPMCAS and (*R*)-PZQ-HPMCAS prepared *via* HME and SE exhibited a similar drug release profile, demonstrating that HME is a promising technique for producing PZQ-ASDs. (*R*)-PZQ-HPMCAS appears to be a potential formulation to replace the currently available commercial racemic PZQ mixture, thereby avoiding the side effects and bitter taste associated with the enantiomer (*S*)-PZQ, as well as lowering the patient pill burden.

Conflicts of interest

The authors declare no conflicts of interest. The authors alone are responsible for the content and writing of the paper.

Data availability

The data supporting this article have been included as part of the ESI.†

Acknowledgements

The authors would like to acknowledge the Bill and Melinda Gates Foundation (Seattle, WA) for funding this study through award number INV-042627. Under the grant conditions of the Foundation, a Creative Commons Attribution 4.0 Generic License has already been assigned to the Author Accepted Manuscript version that might arise from this submission. Mingxin Qian and Tongli Biomedical Co. are thanked for supplying (*R*)-PZQ.

References

1 X. Y. Wang, *et al.*, Prevalence and correlations of schistosomiasis mansoni and schistosomiasis haematobium among humans and intermediate snail hosts: a systematic review and meta-analysis, *Infect. Dis. Poverty*, 2024, **13**(1), 63.
2 K. Mekete, *et al.*, The Geshiyaro Project: a study protocol for developing a scalable model of interventions for moving towards the interruption of the transmission of soil-transmitted helminths and schistosome infections in the Wolaita zone of Ethiopia, *Parasites Vectors*, 2019, **12**(1), 503.
3 World Health Organization, Schistosomiasis, 2025, Available from: **https://www.who.int/news-room/fact-sheets/detail/schistosomiasis** [2023 February 18th].
4 W. H.Organization, *WHO model list of essential medicines: 23rd list, 2023*, World Health Organization, 2023.
5 A. Gaggero, *et al.*, Co-grinding with surfactants as a new approach to enhance in vitro dissolution of praziquantel, *J. Pharm. Biomed. Anal.*, 2020, **189**, 113494.
6 A. Borrego-Sánchez, *et al.*, Molecular and crystal structure of praziquantel. Spectroscopic properties and crystal polymorphism, *Eur. J. Pharm. Sci.*, 2016, **92**, 266–275.
7 E. D. Costa, *et al.*, Unexpected solvent impact in the crystallinity of praziquantel/poly(vinylpyrrolidone) formulations. A solubility, DSC and solid-state NMR study, *Int. J. Pharm.*, 2016, **511**(2), 983–993.
8 D. N. O. Kuevi, *et al.*, Challenges and Proven Recommendations of Praziquantel Formulation, *J. Clin. Pharm. Ther.*, 2023, **2023**(1), 3976392.
9 F. C. Lombardo, B. Perissutti and J. Keiser, Activity and pharmacokinetics of a praziquantel crystalline polymorph in the Schistosoma mansoni mouse model, *Eur. J. Pharm. Biopharm.*, 2019, **142**, 240–246.
10 A. Borrego-Sánchez, *et al.*, Praziquantel–Clays as Accelerated Release Systems to Enhance the Low Solubility of the Drug, *Pharmaceutics*, 2020, **12**(10), 914.
11 T. K. Špehar, *et al.*, Investigation of Praziquantel/Cyclodextrin Inclusion Complexation by NMR and LC-HRMS/MS: Mechanism, Solubility, Chemical Stability, and Degradation Products, *Mol. Pharm.*, 2021, **18**(11), 4210–4223.
12 P. L. Bonate, *et al.*, Extrapolation of praziquantel pharmacokinetics to a pediatric population: a cautionary tale, *J. Pharmacokinet. Pharmacodyn.*, 2018, **45**(5), 747–762.
13 P. Olliaro, P. Delgado-Romero and J. Keiser, The little we know about the pharmacokinetics and pharmacodynamics of praziquantel (racemate and R-enantiomer), *J. Antimicrob. Chemother.*, 2014, **69**(4), 863–870.
14 I. D'Abbrunzo, G. Procida and B. Perissutti, Praziquantel Fifty Years on: A Comprehensive Overview of Its Solid State, *Pharmaceutics*, 2024, **16**(1), 27.
15 T. Meyer, *et al.*, Taste, A New Incentive to Switch to (R)-Praziquantel in Schistosomiasis Treatment, *PLoS Neglected Trop. Dis.*, 2009, **3**(1), e357.
16 S.-K. Park, *et al.*, Mechanism of praziquantel action at a parasitic flatworm ion channel, *Sci. Transl. Med.*, 2021, **13**(625), eabj5832.
17 R. Iyer, *et al.*, Amorphous Solid Dispersions (ASDs): The Influence of Material Properties, Manufacturing Processes and Analytical Technologies in Drug Product Development, *Pharmaceutics*, 2021, **13**(10), 1682.
18 J. A. Baird and L. S. Taylor, Evaluation of amorphous solid dispersion properties using thermal analysis techniques, *Adv. Drug Delivery Rev.*, 2012, **64**(5), 396–421.

19 A. K. P. Mann, *et al.*, Producing Amorphous Solid Dispersions via Co-Precipitation and Spray Drying: Impact to Physicochemical and Biopharmaceutical Properties, *J. Pharm. Sci.*, 2018, **107**(1), 183–191.
20 S. Mohapatra, *et al.*, Effect of Polymer Molecular Weight on the Crystallization Behavior of Indomethacin Amorphous Solid Dispersions, *Cryst. Growth Des.*, 2017, **17**(6), 3142–3150.
21 A. Budiman, *et al.*, Effect of Drug–Polymer Interaction in Amorphous Solid Dispersion on the Physical Stability and Dissolution of Drugs: The Case of Alpha-Mangostin, *Polymers*, 2023, **15**(14), 3034.
22 C. S. Ferreira Marques, *et al.*, Solid dispersion of praziquantel enhanced solubility and improve the efficacy of the schistosomiasis treatment, *J. Drug Delivery Sci. Technol.*, 2018, **45**, 124–134.
23 K. Zheng, *et al.*, Effect of Particle Size and Polymer Loading on Dissolution Behavior of Amorphous Griseofulvin Powder, *J. Pharm. Sci.*, 2019, **108**(1), 234–242.
24 Y. Liu, *et al.*, Dissolution and oral bioavailability enhancement of praziquantel by solid dispersions, *Drug Delivery Transl. Res.*, 2018, **8**(3), 580–590.
25 P. Torre, S. Torrado and S. Torrado, Preparation, Dissolution and Characterization of Praziquantel Solid Dispersions, *Chem. Pharm. Bull.*, 1999, **47**, 1629–1633.
26 S. Orlandi, *et al.*, Structural Elucidation of Poloxamer 237 and Poloxamer 237/Praziquantel Solid Dispersions: Impact of Poly(Vinylpyrrolidone) over Drug Recrystallization and Dissolution, *AAPS PharmSciTech*, 2018, **19**(3), 1274–1286.
27 N. El-Lakkany, S. H. S. el-Din and L. Heikal, Bioavailability and in vivo efficacy of a praziquantel–polyvinylpyrrolidone solid dispersion in Schistosoma mansoni-infected mice, *Eur. J. Drug Metab. Pharmacokinet.*, 2012, **37**(4), 289–299.
28 P. R. Dametto, *et al.*, Development and physicochemical characterization of solid dispersions containing praziquantel for the treatment of schistosomiasis, *J. Therm. Anal. Calorim.*, 2017, **127**(2), 1693–1706.
29 M. V. Chaud, *et al.*, Solid dispersions with hydrogenated castor oil increase solubility, dissolution rate and intestinal absorption of praziquantel, *Braz. J. Pharm. Sci.*, 2010, **46**, 473–481.
30 M. V. Chaud, *et al.*, Development and Evaluation of Praziquantel Solid Dispersions in Sodium Starch Glycolate, *Trop. J. Pharm. Res.*, 2013, **12**, 163–168.
31 M. Cugovčan, *et al.*, Biopharmaceutical characterization of praziquantel cocrystals and cyclodextrin complexes prepared by grinding, *J. Pharm. Biomed. Anal.*, 2017, **137**, 42–53.
32 M. Münster, *et al.*, Multiparticulate system combining taste masking and immediate release properties for the aversive compound praziquantel, *Eur. J. Pharm. Sci.*, 2017, **109**, 446–454.
33 J. Boniatti, *et al.*, Direct Powder Extrusion 3D Printing of Praziquantel to Overcome Neglected Disease Formulation Challenges in Paediatric Populations, *Pharmaceutics*, 2021, **13**(8), 1114.
34 U. Bhatt, U. S. Murty and S. Banerjee, Theoretical and experimental validation of praziquantel with different polymers for selection of an appropriate matrix for hot-melt extrusion, *Int. J. Pharm.*, 2021, **607**, 120964.
35 S. Klein, The use of biorelevant dissolution media to forecast the in vivo performance of a drug, *AAPS J.*, 2010, **12**(3), 397–406.
36 T. Eason, *et al.*, Revisiting the Dissolution of Praziquantel in Biorelevant Media and the Impact of Digestion of Milk on Drug Dissolution, *Pharmaceutics*, 2022, **14**(10), 2228.
37 European Pharmacopoeia Commission, Recommendations on Methods for Dosage Forms Testing, in *European Pharmacopoeia*, European Directorate for the Quality of Medicines (EDQM), Strasbourg, 2014.
38 Biorelevant, Which Ingredients Are in FeSSIF-V2 Powder? n.d. February 26, 2025; available from: **https://biorelevant.com/learning_center/Which-ingredients-are-fessif-v2-powder/**.
39 G. A. Ilevbare and L. S. Taylor, Liquid–Liquid Phase Separation in Highly Supersaturated Aqueous Solutions of Poorly Water-Soluble Drugs: Implications for Solubility Enhancing Formulations, *Cryst. Growth Des.*, 2013, **13**(4), 1497–1509.
40 M. Qian, *et al.* Crystal form of (R)-Praziquantel and preparation method and application thereof, U.S. Patent No. 9657017, U.S. Patent and Trademark Office, 2017.
41 S. K. El-Arini, D. Giron and H. Leuenberger, Solubility properties of racemic praziquantel and its enantiomers, *Pharm. Dev. Technol.*, 1998, **3**(4), 557–564.
42 H. Polyzois, *et al.*, Amorphous Solid Dispersion Formation for Enhanced Release Performance of Racemic and Enantiopure Praziquantel, *Mol. Pharm.*, 2024, **21**(10), 5285–5296.
43 M. Choudhari, *et al.*, Emerging Applications of Hydroxypropyl Methylcellulose Acetate Succinate: Different Aspects in Drug Delivery and Its Commercial Potential, *AAPS PharmSciTech*, 2023, **24**(7), 188.
44 J. Zhang, *et al.*, Advances in the development of amorphous solid dispersions: The role of polymeric carriers, *Asian J. Pharm. Sci.*, 2023, **18**(4), 100834.
45 R. Holm, A. Müllertz and H. Mu, Bile salts and their importance for drug absorption, *Int. J. Pharm.*, 2013, **453**(1), 44–55.
46 J.-n. Yu, *et al.*, Enhancement of oral bioavailability of the poorly water-soluble drug silybin by sodium cholate/phospholipid-mixed micelles, *Acta Pharmacol. Sin.*, 2010, **31**(6), 759–764.
47 C. Pigliacelli, *et al.*, Interaction of polymers with bile salts – Impact on solubilisation and absorption of poorly water-soluble drugs, *Colloids Surf., B*, 2023, **222**, 113044.
48 Chemaxon, *Playground*, Chemaxon Ltd., Budapest, Hungary, 2025. Available from: **https://playground.calculators.cxn.io/**.
49 N. Castro, *et al.*, Bioavailability of praziquantel increases with concomitant administration of food, *Antimicrob. Agents Chemother.*, 2000, **44**(10), 2903–2904.

50 R. B. Chavan, *et al.*, Evaluation of the inhibitory potential of HPMC, PVP and HPC polymers on nucleation and crystal growth, *RSC Adv.*, 2016, **6**(81), 77569–77576.
51 J. M. Miller, *et al.*, A Win–Win Solution in Oral Delivery of Lipophilic Drugs: Supersaturation via Amorphous Solid Dispersions Increases Apparent Solubility without Sacrifice of Intestinal Membrane Permeability, *Mol. Pharm.*, 2012, **9**(7), 2009–2016.
52 A. Butreddy, Hydroxypropyl methylcellulose acetate succinate as an exceptional polymer for amorphous solid dispersion formulations: A review from bench to clinic, *Eur. J. Pharm. Biopharm.*, 2022, **177**, 289–307.
53 D. D. Shah and L. S. Taylor, Chemistry and ionization of HPMCAS influences the dissolution and solution-mediated crystallization of posaconazole amorphous solid dispersions, *J. Pharm. Sci.*, 2025, **114**(1), 223–233.
54 D. T. Friesen, *et al.*, Hydroxypropyl Methylcellulose Acetate Succinate-Based Spray-Dried Dispersions: An Overview, *Mol. Pharm.*, 2008, **5**(6), 1003–1019.
55 W. Curatolo, J. A. Nightingale and S. M. Herbig, Utility of hydroxypropylmethylcellulose acetate succinate (HPMCAS) for initiation and maintenance of drug supersaturation in the GI milieu, *Pharm. Res.*, 2009, **26**(6), 1419–1431.
56 A. Elkhabaz, *et al.*, Crystallization Kinetics in Fasted-State Simulated and Aspirated Human Intestinal Fluids, *Cryst. Growth Des.*, 2021, **21**(5), 2807–2820.
57 I. Meister, *et al.*, Activity of Praziquantel Enantiomers and Main Metabolites against Schistosoma mansoni, *Antimicrob. Agents Chemother.*, 2014, **58**(9), 5466–5472.
58 X. Wen, *et al.*, Preparation and In Vitro/In Vivo Evaluation of Orally Disintegrating/Modified-Release Praziquantel Tablets, *Pharmaceutics*, 2021, **13**(10), 1567.
59 C. Rodríguez-Ruiz, *et al.*, Structural, Physicochemical, and Biopharmaceutical Properties of Cocrystals with RS- and R-Praziquantel–Generation and Prolongation of the Supersaturation State in the Presence of Cellulosic Polymers, *Cryst. Growth Des.*, 2022, **22**(10), 6023–6038.
60 B. Atawa, *et al.*, Impact of chirality on the Glass Forming Ability and the crystallization from the amorphous state of 5-ethyl-5-methylhydantoin, a chiral poor glass former, *Int. J. Pharm.*, 2018, **540**(1), 11–21.
61 Sigma-Aldrich, Praziquantel. n.d. March 9, 2025; available from: **https://www.sigmaaldrich.com/US/en/product/sigma/p4668**.
62 R. M. Mainardes, M. P. D. Gremião and R. C. Evangelista, Thermoanalytical study of praziquantel-loaded PLGA nanoparticles, *Rev. Bras. Cienc. Farm.*, 2006, **42**, 523–530.
63 M. Qian, *R-Praziquantel Preparation Method*, Suzhou Tongli Biomedical Co., Ltd, United States, 2015.
64 J. M. C. de Assis, *et al.*, Hot-melt extrudability of amorphous solid dispersions of flubendazole-copovidone: An exploratory study of the effect of drug loading and the balance of adjuvants on extrudability and dissolution, *Int. J. Pharm.*, 2022, **614**, 121456.
65 N. Nyamweya and S. W. Hoag, Assessment of polymer-polymer interactions in blends of HPMC and film forming polymers by modulated temperature differential scanning calorimetry, *Pharm. Res.*, 2000, **17**(5), 625–631.
66 A. L. Sarode, *et al.*, Stability assessment of hypromellose acetate succinate (HPMCAS) NF for application in hot melt extrusion (HME), *Carbohydr. Polym.*, 2014, **101**, 146–153.
67 Y. Li, *et al.*, Interactions between drugs and polymers influencing hot melt extrusion, *J. Pharm. Pharmacol.*, 2014, **66**(2), 148–166.
68 G. Verreck, The Influence of Plasticizers in Hot-Melt Extrusion, in Hot–Melt Extrusion, *Pharm. Appl.*, 2012, 93–112.
69 D. K. Tan, *et al.*, Innovations in Thermal Processing: Hot-Melt Extrusion and KinetiSol® Dispersing, *AAPS PharmSciTech*, 2020, **21**(8), 312.
70 S. Tambe, *et al.*, Hot-melt extrusion: Highlighting recent advances in pharmaceutical applications, *J. Drug Delivery Sci. Technol.*, 2021, **63**, 102452.